Marmara Fen Bilimleri Dergisi 2018, 4: 383-387
DOI: 10.7240/marufbd.399357

RESEARCH ARTICLE / ARAŞTIRMA MAKALESİ

Phononic Stability Analysis of Two-Dimensional Carbon Nitride Monolayers

İki-Boyutlu Tek-tabaka Karbon Nitrürlerin Fononik Kararlılık Analizi

Sevil SARIKURT [1], Fatih ERSAN [2]

[1]Dokuz Eylul University, Department of Physics, Faculty of Science, 35390, Izmir, TURKEY
[2]Adnan Menderes University, Department of Physics, 09010, Aydin, TURKEY

Abstract

In this study we examined the dynamical stability and electronic properties of carbon nitrides monolayers as C_6N_6 and C_6N_8. We found that buckled form of C_6N_8 monolayer is dynamically stable instead of planar C_6N_8, which has been studied many times in literature. While planar C_6N_8 has negative optical phonon modes, properly created buckling in the structure can make these imaginarities disappear and make the system dynamically stable. In the literature, the planar form of C_6N_6 monolayer is predicted to be stable. In this work, we find out that buckling in the C_6N_6 destabilizes the out-of-plane transverse acoustic mode (ZA) and the soft mode of the optical branch. Both buckled C_6N_8 and planar C_6N_6 have direct band gap of 1.82 eV and 1.58 eV, respectively, which fall in the visible region. Our outcomes may be useful in fabricating optical devices that operate in the visible range of the spectrum.

Keywords: Carbon nitrides, monolayer, 2D materials, density functional theory, phonon.

Öz

Bu çalışmada, tek tabakalı C_6N_6 and C_6N_8 karbon nitrürlerin dinamik kararlılıklarını ve elektronik özelliklerini inceledik. Literatürde bir çok kez çalışılmış olan düzlemsel C_6N_8 yerine, bükülmüş tek-tabakalı C_6N_8'in dinamik olarak kararlı olduğunu bulduk. Düzlemsel C_6N_8, negatif optik fonon modlarına sahipken, yapıda uygun bir şekilde oluşturulan bükülme bu imajinerliklerin ortadan kalkmasını ve sistemin dinamik olarak kararlı olmasını sağlamaktadır. Literatürde, tek tabakalı C_6N_6'nın düzlemsel formunun kararlı olduğu bulunmuştur. Bu çalışmada, C_6N_6'daki bükülmenin, düzlem-dışı enine akustik modun (ZA) ve optik dalın yumuşak modunun kararlılıklarını bozduğunu ortaya çıkardık. Hem bükülmüş C_6N_8 hem de düzlemsel C_6N_6, görünür bölge icinde olan sırasıyla 1.82 eV ve 1.58 eV dogrudan bant aralığına sahiptir. Bizim sonuçlarımız, spektrumun görünür bölge aralığında çalışan optik cihazların üretiminde faydalı olabilir.

Anahtar Kelimeler: Karbon nitrütler, tek-tabaka, 2B malzemeler, yoğunluk fonksiyoneli teorisi, fonon.

I. INTRODUCTION

Graphitic carbon nitrides attract great interest due to they can break off hydrogen from water under sunlight irradiation [1]. Several experimental studies focus on the synthesization and characterization polymorphs of carbon nitrides [2-5]. Recently, Pan et. al have reported that the graphitic carbon nitride nanotubes are promising materials for solar energy absorbers due to their size-dependent bandgaps [6]. And also they have revealed that electronic and optical properties of the carbon nitride nanotubes can be easily tuned via adsorption of metal adatoms [6]. Ma et. al have showed that photoactivity of C_6N_8 carbon nitride allotrope can be enhanced via nonmetal atom doping and at the end of the functionalization process, the property of visible-light absorbtion of C_6N_8 has been increased [7]. These materials have been also investigated for helium detection and it is obtained that C_6N_8 membrane has high capability to separate He from other gas molecules such as H_2, N_2, CO and CH_4 [8]. Researchers have proposed several new types of carbon nitride membranes by theoretical calculations [9-11], and some of these membranes have already been

Sorumlu Yazar/Corresponding Author: Fatih ERSAN, **Tel:** +902562128498**, e-posta:** fatih.ersan@adu.edu.tr
Gönderilme/Submitted: 25.02.2018, **Düzenleme/Revised:** 11.09.2018, **Kabul/Accepted:** 06.11.2018

synthesized [12]. But among them mostly interested ones are C_6N_6 and C_6N_8 monolayers [13-18]. The synthesization, detailed structural characterization and stability of bulk graphitic C_6N_6 and C_3N_4 structures have been reported by several researchers [19-21]. All above-mentioned theoretical studies investigated planar carbon nitrides and their interaction with adatom or molecules, but few of them examine the stabilities of the structures by cohesive or formation energy calculations [22,23]. However, as is known the phonon dispersion calculation is one of the most important stability analysis, because of, in spite of the structure can has a large cohesive energy, it can be dynamically unstable. So, in this study we have investigated dynamical stability of the two-dimensional planar/buckled C_6N_6 and C_6N_8 monolayers using first principles calculations. Our simulations indicate that, although planar C_6N_6 is stable, its buckled form is not. On the contrary, buckled form of C_6N_8 monolayer is stable, while its planar form is unstable.

II. COMPUTATIONAL METHOD

In order to investigate the dynamical stability and electronic properties of the carbon nitride monolayers, we employ spin-unpolarised plane-wave calculations within density functional theory (DFT) using the Perdew, Burke, and Ernzerhof (PBE) parametrization [24] and Vanderbilt ultrasoft pseudopotential method implemented in Quantum Espresso (QE) software [25]. Generalized gradient approximation (GGA) is used for exchange-correlation function. Kinetic energy cutoff parameter for plane-wave basis set is taken to be 80 Ry. Monkhorst-Pack method with 9 x 9 x 1 **k**-points mesh is used to sample the Brillouin Zone [26]. Broyden-Fletcher-Goldfarb-Shanno (BFGS) iterative method is used to optimize the structures [27]. At the end of the optimization procedure, we obtained Hellmann-Feynman forces acting on each atom are less than 0.04 eV/Å. Total energy difference between the successive iteration is set to 10^{-6} Ry. Gaussian smearing method is used with a smearing width of 0.001 Ry. To create monolayer carbon nitride structure, vacuum length is set to 20 Å. Phonon band structures of the C_6N_6 and C_6N_8 monolayers are obtained by using QE software, which implements the density functional perturbation theory (DFPT). For these calculations, 10^{-14} (a.u) is set for threshold for self-consistency. For the phonon calculation on the uniform grid of q-points, 4 x 4 x 1 Monkhorst-Pack grid is chosen. The average cohesive energy is obtained by using below equation

$$E_{coh} = (nE_C + mE_N - E_{CnNm}) / (n+m)$$

where E_{CnNm} is the total energy of the carbon nitride structure and E_C and E_N are the total energies of the isolated carbon and nitrogen atoms, respectively. The numbers of the C and N atoms in the unitcell are illustrated by n and m, respectively.

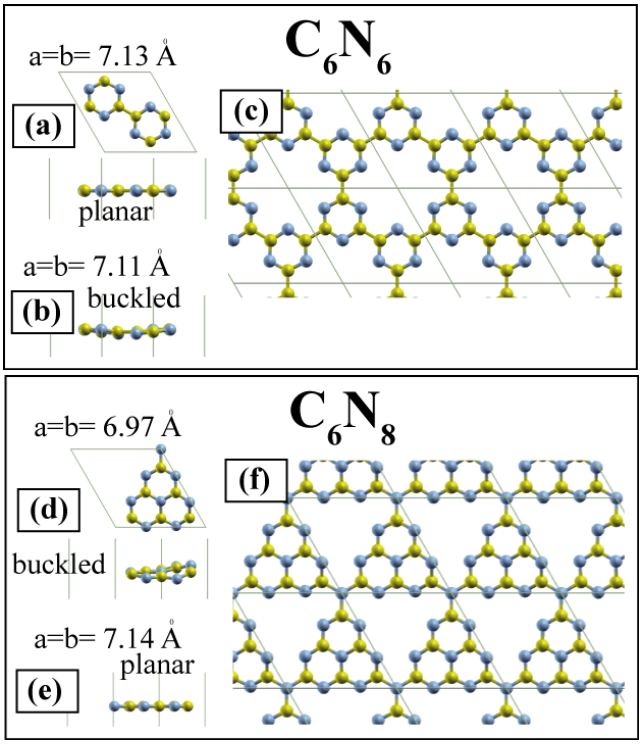

Figure 1. a) Top and side view of planar C_6N_6 monolayer, also lattice constants are given, b) side view of buckled C_6N_6, c) Extended top view of planar C_6N_6 structure, d) top and side view of buckled C_6N_8 monolayer, also lattice constants are given, b) side view of planar C_6N_8, c) Extended top view of planar C_6N_8 structure.

III. RESULTS AND DISCUSSIONS

We first constructed 1x1 carbon nitrides monolayers as illustrated in Figure 1. For each carbon nitrides both planar and buckled structures are created. Figure 1 (a) , (b) and (c) represents the top and side views of C_6N_6 monolayer. The obtained lattice parameters for planar C_6N_6 are a=b=7.13 Å, while values of a=b=7.11 Å are found for buckled structure. Planar C_6N_6 has two hexagons in the unitcell with 1.34 Å C-N bond length and these two hexagons bind each other from carbon atoms with of 1.51 Å C-C bond distance. Every six C_3N_3 hexagons surround a pore as illustrated in Figure 1 (c) and the diameter of the pore is 5.48 Å. To form the buckled structure of C_6N_6, some edge atoms in the unitcell have been raised up until the maximum height is reached to 0.30 Å above from the other atoms in z-direction. After optimization, calculated total energy difference between the two C_6N_6 structures is 0.110 eV, and planar one has minimum ground state energy. Calculated the average cohesive energy of planar C_6N_6 is 0.442 eV per atom. Figure 1 (d), (e), and (f) illustrate the top and side views of buckled and planar C_6N_8 monolayer structures.

Lattice parameters of planar C_6N_8 structure are little larger than planar C_6N_6 and are a=b=7.14 Å, while buckled one are a=b=6.97 Å. Ground state energy difference between the buckled and planar C_6N_8 structures is obtained as 0.331 eV and buckled form is predicted as energetically favorable structure for C_6N_8 in contradiction to the C_6N_6 structure. Corresponding average cohesive energy of buckled C_6N_8 is 0.429 eV per atom. Buckling distance is 1.05 Å from the highest atom to the lowest atom in z-direction. C_6N_8 structures, C-N bond lengths vary between 1.29-1.45 Å. All these calculated results are in good agreement with previous studies [13-16,21-23]. Cohesive energy calculation is a way to determine the stability of a structure by evaluating the cohesion strength between the constituent atoms in the cell. But this method is not enough to analyze the stability, because that structure could be in a local minimum on the Born-Oppenheimer surface. To clarify this point, we checked their dynamical stabilities by phonon frequency calculations along the whole Brillouin Zone using QE code with the help of DFPT. The phonon band structures of planar and buckled C_6N_6 structures are given in Figure 2 (a), as seen there is not any imaginary phonon frequency for planar C_6N_6.

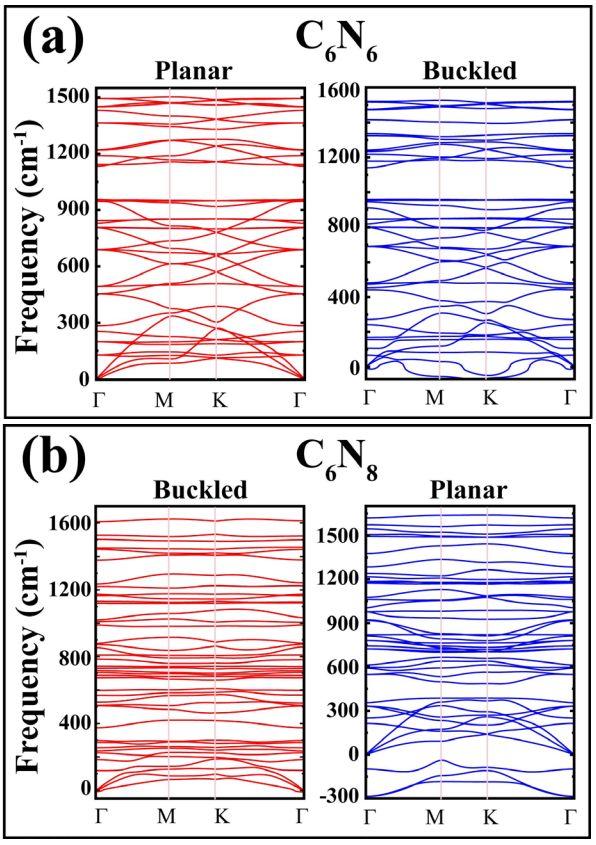

Figure 2. Phonon band structures of buckled and planar a) C_6N_6 and b) C_6N_8 monolayers, stable ones are red colored.

The dynamical stability of planar C_6N_6 has also been determined by Wang et al. from first-principles calculations and molecular dynamics simulations [18]. Our obtained phonon spectrum is compatible with their results. In addition to this, we have also investigated the phonon dispersion curves of buckled form of C_6N_6 structure. There are thirty-six separated phonon branches for C_6N_6 structures, which include thirty-three optical and three acoustical branches. Buckling in the C_6N_6 unitcell results structural instability and one of the acoustical branch, which is the out of plane (ZA), and one optical branch (soft mode of optical branch) have imaginary frequencies. In contradiction to C_6N_6, buckled form of C_6N_8 shows dynamical stability (please see Figure 2 (b)). The phonon dispersion of planar form of C_6N_8 structure has large imaginary frequencies for optical modes, while its three acoustical phonon branches have positive values. This situation implies that some atoms in the cell want to raise up from their atomic positions. Hence, we changed their coordinates and created buckling in the cell as mentioned above part, at the end of the optimization C_6N_8 monolayer gains dynamical stability as shown in Figure 2 (b). Three negative optical branches in the planar C_6N_8, go up to approximately 200 cm^{-1} and therefore, buckled C_6N_8 has forty-two positive phonon modes. In Figure 3 (a) and (b), we present the electronic band, band decomposed charge densities (BDCD) at the K high symmetry point and partial density of states (PDOS) of stable planar C_6N_6 and buckled C_6N_8 monolayers. Both of carbon nitrides structures have direct band gap of 1.58 eV for C_6N_6 and 1.82 eV for C_6N_8 which are located in the visible region and comparable with previous studies [7,21]. It should be noted that electronic band structures of the considered materials are obtained by standard PBE calculations, which underestimates the band gap value. Probably the calculation with the Heyd-Scuseria-Ernzerhof (HSE06) hybrid functional [28] leads to an increase in their band gap values. For instance, calculated band gap value with the HSE06 is 3.05 eV for the buckled C_6N_8 structure [29]. Furthermore, detailed analysis for the electronic structure and the isosurfaces of the Kohn–Sham wave functions for planar C_6N_6 structure have been reported by Wang et al. [18]. As can be seen from Figure 3(a), three Dirac bands appear in C_6N_6 band structure above and below the Fermi level. As is known from graphene, silicene and germanene, this kind of matching bands can show massless Dirac Fermions properties. But this band matching must be on Fermi level. Accordingly, maybe this Dirac bands can be moved with changing the Fermi level by applying electrical field or by charging the system. The buckled C_6N_8 structure has more flat bands according to planar C_6N_6 structure. This could be due to the effect of buckling and so localize bands

occur in the electronic band structure. As can be seen from the BDCD, charges are localized on the whole atoms in the unitcells for the conduction band minimums. Dirac points in the C_6N_6 band structure consist of the p_x and p_y orbitals of the Nitrogen atoms. According to Lowdin analysis, each nitrogen atom receives 0.21 electrons from carbon atoms in the C_6N_6 structure. For C_6N_8, each carbon atom loses 0.40 electrons and nitrogene atoms share these electrons between them and each one takes 0.30 electrons. As can be seen in PDOS figures, *p*-orbitals of nitrogene atoms dominate valence band maximums for both systems and a little contribution comes from the *s*-orbital of nitrogene atoms. Conduction band minimums for both carbon nitrides occupied by *p*-orbitals of C and N atoms.

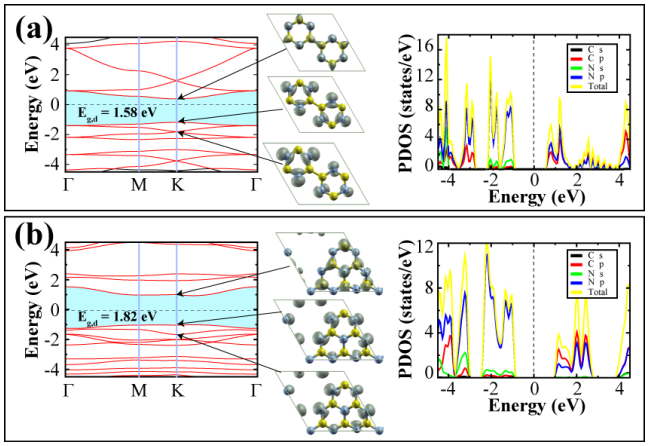

Figure 3. a) Electronic band structure and partial density of states (PDOS) of planar (stable) C_6N_6 monolayer, b) Electronic band structure and partial density of states (PDOS) of buckled (stable) C_6N_8 monolayer. Band gaps are shaded and gap character is labeled by "d" letter which means direct band gap. Band decomposed charge densities (BDCD) at the K symmetry point are also illustrated.

IV. CONCLUSION

In conclusion, by using first principles calculations we investigated the dynamical stability of two carbon nitrides monolayers. Our results show that planar structure of C_6N_6 is dynamically stable; while C_6N_8 is stable when proper buckling height is created in the structure. The calculated average cohesive energy values are not so large which can imply that their thermal stability could be poor with respect to the graphene, but they could be suitable materials for optical devices operating in the visible region at the room temperature and above it. We believe that with our extensive study, investigations may condense on buckled C_6N_8 structure instead of planar one.

Acknowledgment

Computing resources used in this work were provided by the TUBITAK ULAKBIM, High Performance and Grid Computing Center (Tr-Grid e-Infrastructure).

References

[1] Wang, X., Maeda, K., Thomas, A., Takanabe, K., Xin, G., Carlsson, J. M., and Antonietti, M. (2009). A metal-free polymeric photocatalyst for hydrogen production from water under visible light. *Nature materials*, *8*(1), 76.

[2] Kroke, E., and Schwarz, M. (2004). Novel group 14 nitrides. *Coordination Chemistry Reviews*, *248*(5-6), 493-532.

[3] Fang, L., Ohfuji, H., Shinmei, T., and Irifune, T. (2011). Experimental study on the stability of graphitic C3N4 under high pressure and high temperature. *Diamond and Related Materials*, *20*(5-6), 819-825.

[4] Zou, X. X., Li, G. D., Wang, Y. N., Zhao, J., Yan, C., Guo, M. Y., and Chen, J. S. (2011). Direct conversion of urea into graphitic carbon nitride over mesoporous TiO 2 spheres under mild condition. *Chemical Communications*, *47*(3), 1066-1068.

[5] Jürgens, B., Irran, E., Senker, J., Kroll, P., Müller, H., and Schnick, W. (2003). Melem (2, 5, 8-triamino-tri-s-triazine), an important intermediate during condensation of melamine rings to graphitic carbon nitride: Synthesis, structure determination by X-ray powder diffractometry, solid-state NMR, and theoretical studies. *Journal of the American Chemical Society*, *125*(34), 10288-10300.

[6] Pan, H., Zhang, Y. W., Shenoy, V. B., and Gao, H. (2011). Ab initio study on a novel photocatalyst: functionalized graphitic carbon nitride nanotube. *Acs Catalysis*, *1*(2), 99-104.

[7] Ma, X., Lv, Y., Xu, J., Liu, Y., Zhang, R., and Zhu, Y. (2012). A strategy of enhancing the photoactivity of g-C3N4 via doping of nonmetal elements: a first-principles study. *The Journal of Physical Chemistry C*, *116*(44), 23485-23493.

[8] Li, F., Qu, Y., and Zhao, M. (2015). Efficient helium separation of graphitic carbon nitride membrane. *Carbon*, *95*, 51-57.

[9] Molina, B., and Sansores, L. E. (1999). Electronic structure of six phases of C_3N_4: a theoretical approach. *Modern physics letters B*, *13*(06n07), 193-201.

[10] He, B. L., Shen, J. S., and Tian, Z. X. (2016). Iron-embedded C 2 N monolayer: a promising low-cost and high-activity single-atom catalyst for CO oxidation. *Physical Chemistry Chemical Physics*, *18*(35), 24261-24269.

[11] Tang, X., Hao, J., and Li, Y. (2015). A first-principles study of orthorhombic CN as a potential superhard material. *Physical Chemistry Chemical Physics*, *17*(41), 27821-27825.

[12] Stavrou, E., Lobanov, S., Dong, H., Oganov, A. R., Prakapenka, V. B., Konôpková, Z., & Goncharov, A. F. (2016). Synthesis of ultra-incompressible sp3-hybridized carbon nitride

with 1: 1 stoichiometry. *Chemistry of Materials*, 28(19), 6925-6933.

[13] Abdullahi, Y. Z., Leong, Y. T., Halim, M. M., Hashim, M. R., Leng, L. T., and Uebayashi, K. (2017). Adsorption of atoms and molecules on s-triazine sheet with embedded manganese atom: First-principles calculations. *Physics Letters A*, *381*(43), 3664-3674.

[14] Abdullahi, Y. Z., Yoon, T. L., Halim, M. M., Hashim, M. R., and Lim, T. L. (2017). Effects of atoms and molecules adsorption on electronic and magnetic properties of s-triazine with embedded Fe atom: DFT investigations. *Philosophical Magazine*, 1-16.

[15] Abdullahi, Y. Z., Yoon, T. L., Halim, M. M., Hashim, M. R., and Lim, T. L. (2017). Theoretical studies on mechanical and electronic properties of s-triazine sheet. *Philosophical Magazine*, *97*(24), 2077-2088.

[16] Abdullahi, Y. Z., Yoon, T. L., Halim, M. M., Hashim, M. R., and Lim, T. L. (2018). First-principles investigation of graphitic carbon nitride monolayer with embedded Fe atom. *Surface Science*, *667*, 112-120.

[17] Kroke, E., Schwarz, M., Horath-Bordon, E., Kroll, P., Noll, B., and Norman, A. D. (2002). Tri-s-triazine derivatives. Part I. From trichloro-tri-s-triazine to graphitic C_3N_4 structures. *New Journal of Chemistry*, *26*(5), 508-512.

[18] Wang, A., Zhang, X., & Zhao, M. (2014). Topological insulator states in a honeycomb lattice of s-triazines. Nanoscale, 6(19), 11157-11162.

[19] Li, J., Cao, C., Hao, J., Qiu, H., Xu, Y., and Zhu, H. (2006). Self-assembled one-dimensional carbon nitride architectures. *Diamond and related materials*, *15*(10), 1593-1600.

[20] Thomas, A., Fischer, A., Goettmann, F., Antonietti, M., Müller, J. O., Schlögl, R., and Carlsson, J. M. (2008). Graphitic carbon nitride materials: variation of structure and morphology and their use as metal-free catalysts. *Journal of Materials Chemistry*, *18*(41), 4893-4908.

[21] Ma, Z., Zhao, X., Tang, Q., and Zhou, Z. (2014). Computational prediction of experimentally possible g-C3N3 monolayer as hydrogen purification membrane. *International Journal of Hydrogen Energy*, *39*(10), 5037-5042.

[22] Deifallah, M., McMillan, P. F., and Cora, F. (2008). Electronic and structural properties of two-dimensional carbon nitride graphenes. *The Journal of Physical Chemistry C*, *112*(14), 5447-5453.

[23] Ji, Y., Dong, H., Lin, H., Zhang, L., Hou, T., and Li, Y. (2016). Heptazine-based graphitic carbon nitride as an effective hydrogen purification membrane. *RSC Advances*, *6*(57), 52377-52383.

[24] Perdew, J. P., Burke, K., and Ernzerhof, M. (1996). Generalized gradient approximation made simple. *Physical Review Letters*, *77*(18), 3865.

[25] Giannozzi, P., Baroni, S., Bonini, N., Calandra, M., Car, R., and Cavazzoni, C., et. al., (2009). QUANTUM ESPRESSO: a modular and open-source software project for quantum simulations of materials. *Journal of Physics: Condensed Matter*, *21*(39), 395502.

[26] Monkhorst, H. J., and Pack, J. D. (1976). Special points for Brillouin-zone integrations. *Physical Review B*, *13*(12), 5188.

[27] Broyden, C. G. (1970). The convergence of a class of double-rank minimization algorithms 1. General considerations. *IMA Journal of Applied Mathematics*, *6*(1), 76-90.

[28] Hummer, K., Harl, J., and Kresse, G. (2009). Heyd-Scuseria-Ernzerhof hybrid functional for calculating the lattice dynamics of semiconductors. *Physical Review B*, 80(11), 115205.

[29] Wu, H-Z., Liu, L-M., and Zhao, S-J, The effect of water on the structural, electronic and photocatalytic properties of graphitic carbon nitride, *Phys. Chem. Chem. Phys.*, 2014, 16, 3299.